

Diffractive processes in pp collisions at 7 TeV measured with the CMS experiment.

Grzegorz Brona^{*†}

Author University of Warsaw

E-mail: grzegorz.brona@cern.ch

CMS results on the single and double diffractive dissociation in proton-proton collisions at $\sqrt{s} = 7$ TeV are presented. The cross sections for both processes are being calculated and compared with previous LHC and non-LHC measurements. The comparison with phenomenological models is also presented with a focus on the PYTHIA8-MBR which describes the data best. Both cross sections tend to raise weakly with the energy. The results give an insight into mechanism of the Pomeron exchange and will improve modeling of diffraction in event generators.

The XXIII International Workshop on Deep Inelastic Scattering and Related Subjects

April 27 - May 1, 2015

Southern Methodist University

Dallas, Texas 75275

^{*}Speaker.

[†]For the CMS Collaboration.

1. Introduction

Diffractive interactions account for about 25% of the total inelastic proton-proton cross section. They are mediated by a color-singlet object carrying vacuum quantum numbers, called Pomeron. The signature of the diffraction is an appearance of at least one large rapidity gap (LRG) in the final state, experimentally detected as a region in pseudorapidity without any activity. There are three main types of diffractive processes. Single dissociation (SD) in which one of the proton taking part in the interaction dissociates and the second stays intact. The process is characterised by an existence of a LRG at one side of the detector, while the other side, if only the diffractive mass is large enough, is populated by particles from the dissociation. Double dissociation (DD) when both protons dissociate and the LRG is located between the two areas populated by the particles. Central diffraction (CD) which technically is a Pomeron-Pomeron interaction and is leading to the creation of the central system separated from the two intact protons by two LRGs. In this paper both, SD and DD are studied, while for CD the cross section is small and can be neglected.

Compact Muon Solenoid (CMS) is one of the two large, multi-purpose experiments at the Large Hadron Collider (LHC) at CERN [1]. The barrel and endcaps coverage of the CMS detector spans to $|\eta| < 3$, while at higher rapidities Hadronic Forward (HF) calorimeter provides acceptance in $3.0 < |\eta| < 5.2$ range. It consists of steel absorbers with embedded radiation hard quartz fibers, providing fast collection of Cherenkov light. At one side of the CMS the CASTOR calorimeter is located. It covers the very forward angles corresponding to $-6.6 < \eta < -5.2$. For the triggering purpose the Beam Scintillator Counters (BSC) and the Beam Pick-up Timing eXperiment (BPTX) are used. The BSC detectors are located at both sides of the interaction point and are sensitive for charged particles in the $3.23 < \eta < 4.65$ range. Their average sensitivity for a minimal ionizing particle detection is 96.3%. The BPTX system provides measurement of the proton bunch structure. The wide geometrical coverage of the experiment and the minimum bias trigger makes the CMS detector a very good tool for the studies of the soft diffraction processes, in which areas devoided of any particles are to be precisely measured.

The analysis presented here is based on the $\sqrt{s} = 7$ TeV proton-proton collisions data, collected by the CMS in 2010 during a low pileup run [2]. The integrated luminosity of $16.2 \mu\text{b}^{-1}$ with an average of $\mu = 0.14$ inelastic pp collisions per bunch crossing is used. The events are selected by triggering on a signal from both BPTX and an activity in at least one of the BSC detectors. These conditions form a well defined minimum bias trigger. Offline, the additional requirement on at least two particles reconstructed within the BSC acceptance is imposed, while no vertex requirement is used which extends the acceptance in the direction of the low diffractive masses ($M_X < 100$ GeV).

In the presented analysis Monte Carlo models are used twice. First, to correct the detector level distribution back to the hadron level observables. This includes the corrections for geometrical detector acceptance, resolution and migrations between kinematic bins. For this part the PYTHIA8-MBR Monte Carlo sample is used and a comparison with PYTHIA8-4C is done to study systematics. Second, the Monte Carlo models are used to study non-diffractive (ND), SD and DD contributions to the observed spectra and by doing this to check different approaches to the diffraction modeling. The diffraction in the PYTHIA8-4C is simulated in accord with the Schuler-Sjostrand model with rescaling downwards by 10% and 12% the SD and DD components,

respectively. In PYTHIA8-MBR the diffractive components are generated with the use of the MBR (Minimum Bias Rockefeller) model. The MBR model is based on a renormalized Regge theory model, unitarized by interpreting the Pomeron flux as the probability for forming a diffractive rapidity gap. The best data description was achieved setting in the model $\varepsilon = 0.08$ and $\alpha' = 0.25 \text{ GeV}^{-1}$ for the Pomeron trajectory $\alpha(t) = 1 + \varepsilon + \alpha't$ and scaling downwards by 15% the DD component. For the comparison also PYTHIA6-ZZ*, and Monte Carlo models based on the Regge-Gribov phenomenology: PHOJET, QGSJET-II and EPOS LHC are used.

2. Event topologies

Sample of events selected with the minimum bias trigger is dominated by ND events. The particles produced in these events populate the entire η space. To enhance the SD and DD components subsamples can be defined by requiring presence of a LRG in different parts of the CMS detector. Three subsamples are formed: FG1 sample containing events with a gap at the edge of the detector on the positive η side, FG2 with a gap on the negative η side and CG sample with a central gap located around $\eta = 0$. For the FG1 and FG2 the η_{max} and η_{min} variables are introduced. They are defined as the highest (lowest) η of the reconstructed object in the central detector (up to $|\eta| = 4.7$, as most outer rings of HF are not used). For CG, variable describing the width of the central rapidity gap, $\Delta\eta^0 = \eta_{max}^0 - \eta_{min}^0$, is introduced. All the discussed topologies are presented schematically in Fig. 1. The FG1 and FG2 samples are composed of real SD events (SD1, SD2)

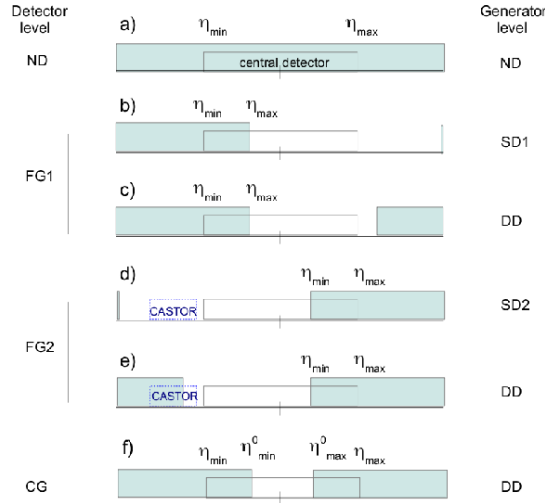


Figure 1: Schematical representation of the FG1, FG2 and CG samples.

and DD events with the low diffractive mass escaping the detectors acceptance. Fig. 2 presents the experimental distributions of the three observables: η_{max} , η_{min} and $\Delta\eta^0$ (blue points). The data are compared to the predictions of PYTHIA-MBR model for different contributions. All the samples are dominated by the ND, with the exponentially suppressed rapidity gaps. The SD and DD contribute dominantly to FG1 and FG2 samples at low η_{max} and high η_{min} . The DD dominates CG at high $\Delta\eta^0$. These correspond to the large sizes of the forward and central LRGs, respectively. Therefore to enhance the diffractive contributions the samples are further restricted with $\eta_{max} < 1$,

$\eta_{min} > -1$ and $\Delta\eta^0 > 3$ cuts.

The FG2 topology can be further decomposed into SD-enhanced and DD-enhanced subsamples. This is done looking for a presence of a signal in the CASTOR detector. If a signal is present, an event is included into the CASTOR-tag sample and in the other case into the no-CASTOR-tag sample. The first of these contains then mostly DD events (with $0.5 < \log_{10}M_Y < 1.1$ GeV, where M_Y stands for a diffractive mass formed at the negative rapidities), while the second mostly SD events with a small admixture of DD events with a diffractive mass too low to produce signal in CASTOR ($\log_{10}M_Y < 0.5$ GeV).

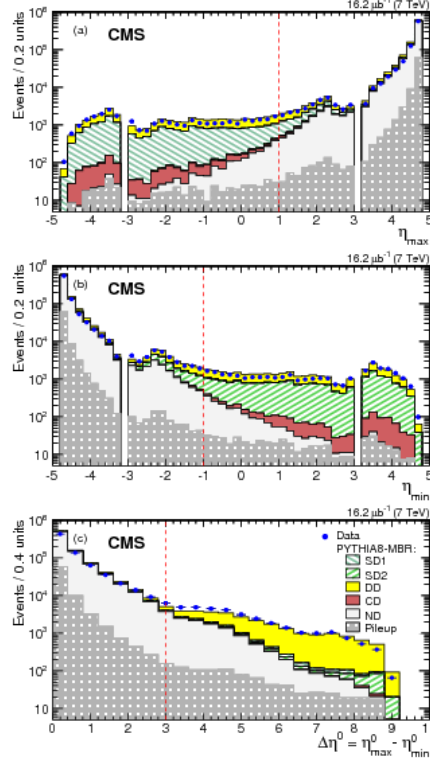


Figure 2: Distributions of η_{max} , η_{min} and $\Delta\eta^0$ variables and comparison with PYTHIA8-MBR predictions for different contributions .

3. Forward and central pseudorapidity gaps cross sections

With the FG2 sample, the forward pseudorapidity gap cross section as a function of ξ_X defined as $\xi_X = M_X^2/s$ is measured. The ξ_X is reconstructed experimentally summing up the energies and longitudinal momenta of all the tracks in an event. This procedure works only in approximation as a fraction of a hadronic system produced in a proton dissociation is contained at large rapidities and escapes through the beam hole. Using PYTHIA8-MBR, a correction factor is introduced, which on an event-by-event bases brings the reconstructed ξ_X to its true value. Finally the differential cross sections are measured in bins of ξ_X for both FG2 subsamples: CASTOR-tag and no-CASTOR-tag. The number of events in each bin is obtained first by counting them directly in the data

and then correcting for acceptance and migration effects. The corrections are calculated with the ROOUNFOLD package, using iterative Bayesian unfolding technique. PYTHIA8-MBR is used to obtain a response matrix for the unfolding. In Fig. 3 the unfolded cross sections are compared with PYTHIA8-MBR, PYTHIA8-4C and PYTHIA6-Z2*. Left plot corresponds to the no-CASTOR-tag while right plot to the CASTOR-tag samples. The best description in both samples is obtained with PYTHIA8-MBR model with $\varepsilon = 0.08$, while PYTHIA8-4C and PYTHIA6-Z2* do not agree with the data.

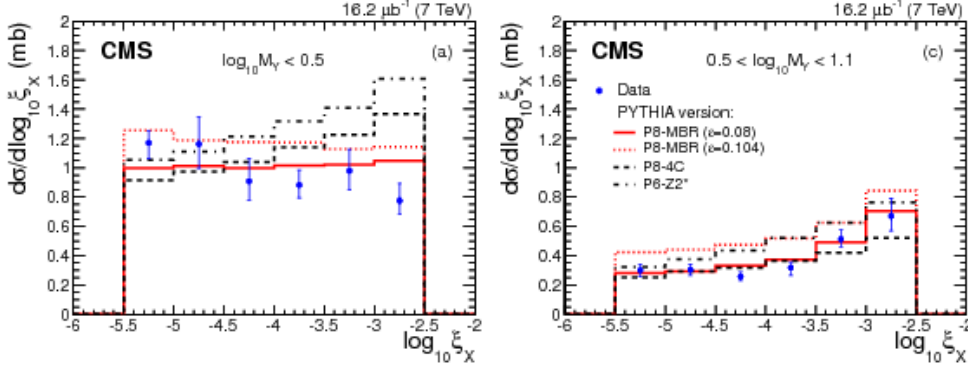


Figure 3: Cross sections for $\log_{10}M_Y < 0.5$ no-CASTOR-tag sample (left) and for $0.5 < \log_{10}M_Y < 1.1$ CASTOR-tag sample (right) and a comparison with predictions from PYTHIA8 and PYTHIA6 models.

The CG sample is used to measure a central pseudorapidity gap cross section as a function of its width, $\Delta\eta$. To translate the measured quantity, $\Delta\eta^0$, to $\Delta\eta$ a calibration factor is introduced. It takes into account detector effects and is extracted from PYTHIA8-MBR. The quoted cross section corresponds to the range of $\Delta\eta > 3$ and $\log_{10}M_{X(Y)} > 1.1$ GeV. The effects of acceptance and migrations between bins are estimated with iterative Bayesian unfolding using PYTHIA8-MBR once again to obtain the response matrix. The measured differential cross section is presented in Fig. 4. The results are compared with PYTHIA8-MBR, PYTHIA8-4C and PYTHIA6-Z2*. PYTHIA8-MBR describes the data best while PYTHIA8-4C underestimates the data in all bins and PYTHIA6-Z2* is below the data in the first $\Delta\eta$ bin.

Finally the integrated cross sections for events containing a forward or central gap are calculated:

- $\sigma_{\text{no-CASTOR-tag}} = 2.99 \pm 0.02(\text{stat})_{-0.29}^{+0.32}(\text{syst})$ mb, $-5.5 < \log_{10}\xi_X < -2.5$ and $0.5 < \log_{10}M_Y < 1.1$
- $\sigma_{\text{CASTOR-tag}} = 1.18 \pm 0.02(\text{stat}) \pm 0.13(\text{syst})$ mb, $-5.5 < \log_{10}\xi_X < -2.5$ and $\log_{10}M_Y < 0.5$
- $\sigma_{\text{CG}} = 0.58 \pm 0.01(\text{stat})_{-0.11}^{+0.13}(\text{syst})$ mb, $\Delta\eta > 3$, $\log_{10}M_Y > 1.1$, $\log_{10}M_Y > 1.1$

4. SD and DD cross sections

From the $\sigma_{\text{no-CASTOR-tag}}$ the SD cross section corresponding to the $-5.5 < \log_{10}\xi_X < -2.5$ is calculated. First the other contributions (ND, DD and CD) in this sample have to be estimated.

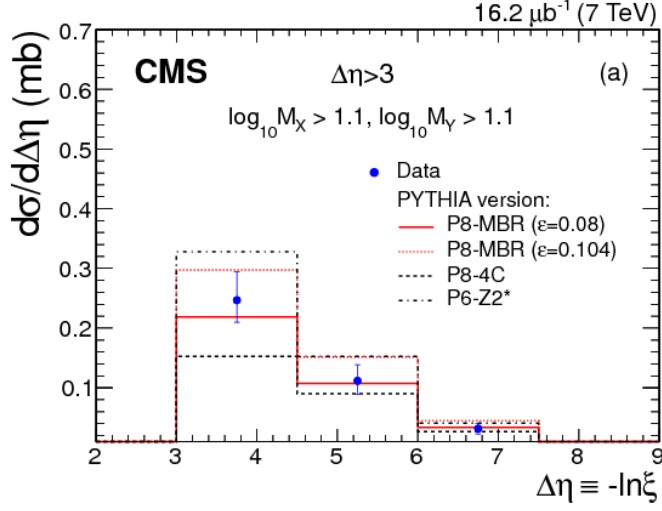


Figure 4: Cross sections for the central rapidity gap cross section in the CG sample (DD dominated) and a comparison with predictions from PYTHIA8 and PYTHIA6 models.

From these the only non-negligible component comes from the DD, the other two are minimal. The DD contribution can be obtained from PYTHIA8-MBR model, and the systematic uncertainty is taken from CASTOR-tag sample where DD events dominate. The uncertainty accounts for the difference between PYTHIA8-MBR predictions for this sample and measured distributions. Finally the $\sigma^{\text{SDVis}} = 4.06 \pm 0.04(\text{stat})_{-0.63}^{+0.69}(\text{syst})$ mb. It corresponds to both $pp \rightarrow Xp$ and $pp \rightarrow pY$.

To calculate the visible cross section for the DD events the following procedure is implemented. First the $\sigma_{\text{CASTOR-tag}}$ and σ_{CG} are corrected for the ND component (the SD and CD contributions are negligible). This is done also using PYTHIA8-MBR and leads to $\sigma_{\text{CASTOR-tag}}^{\text{DDVis}}$ and to $\sigma_{\text{CG}}^{\text{DDVis}}$. Then the $\sigma^{\text{DDVis}} = 2\sigma_{\text{CASTOR-tag}}^{\text{DDVis}} + \sigma_{\text{CG}}^{\text{DDVis}}$ is evaluated. Factor 2 assumes the same dependence of the DD cross section on both sides of CMS. The $\sigma^{\text{DDVis}} = 2.69 \pm 0.04(\text{stat})_{-0.30}^{+0.29}(\text{syst})$.

The comparison of the measured cross sections with the results of other experiments and predictions of the theoretical models requires extrapolation of the σ^{SDVis} to the wider region corresponding to $\xi < 0.05$. Similarly, the σ^{DDVis} has to be extrapolated to $\Delta\eta > 3$. The extrapolation is done using PYTHIA8-MBR. The extrapolation uncertainties are obtained by varying the Pomeron trajectory parameters in PYTHIA8-MBR, α' and ε . The final results are:

- $\sigma^{\text{SD}} = 8.84 \pm 0.08(\text{stat})_{-1.38}^{+1.49}(\text{syst})_{-0.37}^{+1.17}(\text{extr})$ mb, for $\xi_x < 0.05$
- $\sigma^{\text{DD}} = 5.17 \pm 0.08(\text{stat})_{-0.57}^{+0.55}(\text{syst})_{-0.51}^{+1.62}(\text{extr})$ mb, for $\Delta\eta > 3$

In Fig. 5 and 6 the σ^{SD} and σ^{DD} cross sections are compared with previous results and with PYTHIA8-MBR, GLM and KP models. Both cross sections raise weakly with the energy.

5. Pseudorapidity gap cross section

The other approach to study diffraction experimentally is to define the widest pseudorapidity gap that is adjacent to the edge of the detector: $\Delta\eta^{\text{F}} = \max(|\eta_{\text{min}} + 4.7|, |\eta_{\text{max}} - 4.7|)$, where η_{max}

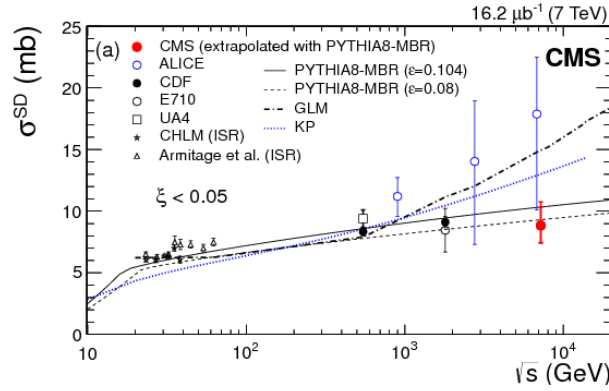


Figure 5: The σ^{SD} as measured by the CMS experiment and comparison with previous measurements and theoretical predictions.

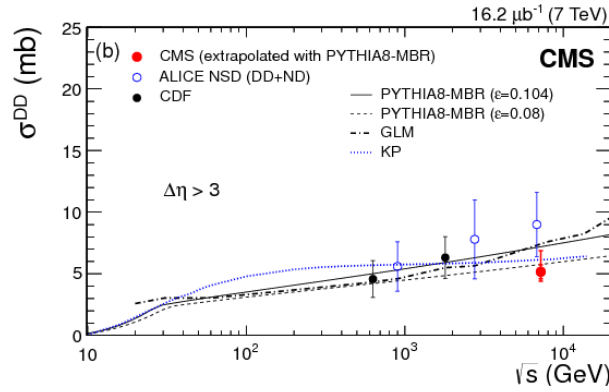


Figure 6: The σ^{DD} as measured by the CMS experiment and comparison with previous measurements and theoretical predictions.

(η_{\min}) is the highest (lowest) η of the reconstructed particle, and 4.7 corresponds to the detector edges. The differential cross section, $d\sigma/d\Delta\eta^F$, is calculated for events with at least one stable final state particle with $p_T > 200$ MeV in $|\eta| < 4.7$. The corrections for migrations are introduced with iterative Bayesian unfolding and PYTHIA8-MBR. The obtained cross section is described very well with the PYTHIA8-MBR.

6. Conclusions

CMS performed a measurement of the σ^{SD} and σ^{DD} . Both cross sections tend to raise weakly with the center of mass energy. The results are compared to measurements from other experiments and models predictions. They add new constrains to the diffraction modeling at the LHC energies.

References

- [1] CMS Collaboration, "The CMS experiment at the CERN LHC", JINST 3 (2008) S08004
- [2] CMS Collaboration, "Measurement of diffraction dissociation cross sections in pp collisions at $\sqrt{s} = 7$ TeV", CMS-FSQ-12-005, CERN-PH-EP-2015-062, submitted to Physical Review D